International Journal of Biological Macromolecules xxx (2013) xxx–xxx

Contents lists available at SciVerse ScienceDirect

International Journal of Biological Macromolecules

journal homepage: www.elsevier.com/locate/ijbiomac

Selective adsorption of Pb(II), Cd(II), and Ni(II) ions from aqueous solution using chitosan–MAA nanoparticles

Aghdas Heidari [a], Habibollah Younesi [a,*], Zahra Mehraban [b], Harri Heikkinen [c]

[a] Department of Environmental Science, Faculty of Natural Resources, Tarbiat Modares University, Imam Reza Street, Noor, Mazandaran Province, PO Box: 46414-356, Iran
[b] New Technologies Committee, Research Institution for Curriculum Development and Educational Innovations, Tehran 158 463 4818, Iran
[c] VTT Technical Research Centre of Finland, Biologinkuja 7, PO Box 1000, Espoo, 02044 VTT, Finland

ARTICLE INFO

Article history:
Received 1 April 2013
Received in revised form 9 May 2013
Accepted 22 June 2013
Available online xxx

Keywords:
Chitosan–MAA nanoparticle
Adsorption isotherm
Kinetics
Desorption

ABSTRACT

Chitosan–MAA nanoparticles (CS–MAA) with an average size of 10–70 nm were prepared by polymerizing chitosan with methacrylic acid in aqueous solution. The physicochemical properties of nanoparticles were investigated using Fourier transform infrared spectroscopy (FT-IR), scanning electron microscopy (SEM), X-ray photoelectron spectroscopy (XPS), dynamic light scattering (DLS) and nuclear magnetic resonance (NMR). The adsorption of Pb(II), Cd(II) and Ni(II) from aqueous solution on CS–MAA was studied in a batch system. The effects of the solution pH, initial metal concentration, contact time, and dosage of the adsorbent on the adsorption process were examined. The experimental data were analyzed using the pseudo-second-order kinetic equations and the Langmuir, Freundlich and Redlish–Peterson isotherms. The maximum adsorption capacity was 11.30, 1.84, and 0.87 mg/g for Pb(II), Cd(II) and Ni(II) ions, respectively, obtained by the Langmuir isotherm. However, the adsorption isotherm was better explained by the Freundlich rather than by the Langmuir model, as the high correlation coefficients ($R^2 > 0.99$) were obtained at a higher confidence level.

© 2013 Published by Elsevier B.V.

1. Introduction

Recently, heavy metals pollution has become the focus of much international attention, mainly because of the voluminous discharge into the environment from industrial activities. Heavy metals are toxic to the ecosystems as well as humans, so their bioaccumulation in the food chain causes serious disorders [1,2]. For example, lead (Pb(II)) may be found in the textile dying, ceramic and glass industries, petroleum refining, battery manufacture and mining operations[3,4]. Pb(II) is categorized as persistent environmental toxic substance and may cause mental disturbance, retardation, and semi-permanent brain damage [5]. Another, cadmium (Cd(II)) is also a risky pollutant coming from metal plating, metallurgical alloying, mining, ceramics and other industrial operations [6]. Cadmium toxicity results in a wide range of syndromes including renal dysfunction, hypertension, hepatic injury, lung damage and teratogenic effects [7]. In addition, nickel (Ni(II)) is commonly used in contemporary industry. Too much exposure of Ni(II) in humans can cause significant influences such as lung, cardiovascular and kidney diseases [8,9].

Methods such as chemical precipitation, reverse osmosis, electrolytic methods of membrane filtration, solvent extraction, ion exchange and adsorption [10,11] have been used for the reduction of heavy metals and recovery from wastewater regarding, which well-known adsorbents such as activated carbon, zeolites, tree bark, biomass, lignin, dried mushrooms, and chitosan have been studied [12,13]. Among the different techniques, adsorption is highly effective because of the ease of operation and its low cost [14].

Chitosan is a biopolymer obtained from natural resources, a partially de-acetylated product of chitin. Chitin is an advantageous compound easily obtainable (from the exoskeleton of shellfish as waste product of the seafood industry), biocompatible, nontoxic, and with antimicrobial properties. In addition, chitosan can chelate heavy metal ions and is therefore a suitable material to be used in heavy metal removal processes [15]. Chitosan is a linear homopolymer formed by β-(1,4)-linked glucosamine units, with reactive hydroxyl and amino groups that can act as substrate for a variety of chemical modifications. These modifications can produce appropriate materials for different medical and industrial purposes. For most heavy metals, chitosan-based sorbents have demonstrated high removal efficiency and sorption kinetics because of the presence of amine groups as chelation sites [16]. Furthermore, physical and chemical modifications have been shown to increase the capacity of chitosan for metal ions sorption selectively [17,18].

* Corresponding author. Tel.: +98 122 625 3101x3; fax: +98 122 625 3499.
E-mail addresses: hunesi@yahoo.com, hunesi@modares.ac.ir (H. Younesi).

0141-8130/$ – see front matter © 2013 Published by Elsevier B.V.
http://dx.doi.org/10.1016/j.ijbiomac.2013.06.032

UNCORRECTED PROOF

Previous studies have illustrated that Cd(II), Ni(II), and Pb(II) ions can be adsorbed from wastewater using chitosan and its derivatives [19–22]. Currently, limited data are available in the literature on the properties of chitosan nanoparticles for heavy metal sorption. Qi and Xu have prepared chitosan nanoparticles by ionic gelation of chitosan and tripolyphosphate (CS–TPP), which have the amine and phosphoric groups as sorption sites for the removal of lead ions from aqueous solution [23]. Haider and Park synthesized chitosan nanofibers by the electrospinning technique and by chemical neutralization of ammonium into an amine group, in order to remove Pb(II) and Cu(II) ions from an aqueous solution [24]. Such data are very helpful and urgently needed, because chitosan nanoparticles have unique characteristics including small size, high surface area, large quantum size per unit mass and wet absorption that is well-suited for adsorption of metal ions.

The objective of this study was to produce chitosan nanoparticles (CS–MAA) by polymerizing methacrylic (MAA) in a chitosan solution. This study reports on adsorption the capacity of CS–MAA for heavy metal ions from aqueous solution. The effects of the pH, the initial metal concentration and the dosage of the adsorbent on the adsorption rate and the adsorption capacity of CS–MAA nanoparticles were evaluated. The adsorption isotherm and sorption kinetics of Ni(II), Cd(II) and Pb(II) ions on CS–MAA are presented.

2. Materials and methods

2.1. Apparatus

Infrared spectra, in the range of 400 to 4000 cm^{-1}, were collected by a Fourier transform infrared (FT-IR) spectroscopy (Shimadzou, FT-IR1650 spectrophotometer, Japan) using KBr powder of spectroscopic quality. The pH value of each solution was adjusted by using a pH meter (Mettler Toledo Instruments Co., Cyberscan, Singapore). The samples were centrifuged (236HK, Hermle, Germany) and a freeze-drier system (Opergn, Korea) was used for lyophilization of the nanoparticles. A scanning electron microscope (SEM, XL30, Philips and Netherlands) was used for characterization of the morphology of CS–MAA nanoparticle and for estimating its particle size. The micrograph of the gold coated CS–MAA nanoparticle was recorded on a field emission scanning electron microscope (SEM) at an electron acceleration voltage of 20 kV. In addition, the particle size distribution was measured by a microstructure measurement and a SEM image. The residual Cd(II), Pb(II) and Ni(II) ions in the adsorption were measured by using an atomic adsorption spectrophotometer (AAS, Philips, PU9400, UK). The ^{13}C NMR measurements were performed with a Chemagnetics CMX 270 MHz infinity NMR spectrometer, with a 6.0 mm double-resonance MAS NMR probe operating at 68.01 MHz. For all the samples, 30,000 transients were accumulated using a 0.5 ms contact time and 2 s recycle time with an MAS rate of 5 kHz. The chemical shifts were referenced to hexamethylbenzene (HMB) using the methyl signal (+17.35 ppm) as an external reference. The average nanoparticle size and the size distribution of CS–MAA was determined by a Malvern Zetasizer analyzer (Malvern Instruments Ltd) using dynamic light scattering (DLS), which determines the nanoparticle size by measuring the distribution of the intensity of the laser light, scattered by nanoparticles as they diffuse through a fluid operating with a 50 mW laser. A suitable amount of distilled water solution of nanoparticles at total concentration of 1% was placed into a quartz cell and measured at a 90° detector angle of, 633 nm wavelength and 25 °C. XPS (X-ray photoelectron spectroscopy) spectra were obtained with 8025-BesTec twin anode XR3E2 X-ray source system (Germany). XPS data were taken using achromatic Mg K_α (1253.6 eV) and Al K_α (1486.6 eV) X-ray source which operated at 15 kV.

2.2. Materials

Chitosan (CS) used in the present study was purchased from Sigma-Aldrich Chemical Co (UK) with deacetylation degrees higher than 85%. Potassium persulfate ($K_2S_2O_8$), methacrylic acid (MAA), HCl and NaOH were purchased from Merck (Darmstadt, Germany) and used without alterations. The Cd(II), Pb(II) and Ni(II) standard solutions were also obtained from the same company. The metal ion solutions for adsorption experiments were prepared by diluting 1000 mg/l of standard solution of Cd(II), Pb(II) and Ni(II) using de-ionized water (Titrisol, Merck, Darmstadt, Germany). The pH of each the heavy metal solution was adjusted by adding diluted NaOH (1 M) or HCl (1 M) using a pH meter (CyberScan, Singapore).

2.3. Synthesis of CS–MAA nanoparticle

The preparation of CS–MAA nanoparticles was done according to the methods of de Moura et al. [25] with slight modification. The nanoparticles were synthesized by polymerizing methacrylic acid in a chitosan solution. Chitosan was dissolved in an aqueous of MAA solution to achieve concentrations of chitosan of 0.25%, 0.5% and 1% (w/w) by magnetic stirring for 12 h. The MAA solution was also dissolved in de-ionized water at 0.5% (w/v). The CS to MAA ratios used in the synthesis were 1:2, 1:1, and 2:1 (w/w, %). The MAA solution was added to the CS solution drop-wise. Afterward, while stirring, 0.2 mmol of $K_2S_2O_8$ was added to the chitosan–methacrylic acid solution for 1.5 h at 70 °C in an N_2 atmosphere. Subsequently, polyampholyte CS–MAA nanoparticles were formed. The formation of the polyampholyte CS–MAA nanoparticle was obtained, because after cross-linking two representative free functional groups of CS–MAA were found. In this case, the residual free amino groups of chitosan were available, which could be protonated in the moderately acidic pH, and the free carboxylic acid groups were available after cross-linking, which could be partially deprotonated in a neutral solution: consequently polyampholyte were obtained. The mixtures were then cooled in an ice bath, and the nanoparticle suspension was centrifuged for 30 min at 4000 rpm and the supernatant was discarded. The particles thus obtained were freeze-dried for 36 h using a freeze-dry system (Opergn, Korea). The resulting freeze-dried CS–MAA nanoparticles were stored in a refrigerator at 4 °C to be used in our adsorption experiments.

2.4. Batch adsorption studies

Adsorption experiments were conducted in 250 ml conical flasks each containing 100 ml of Cd(II), Ni(II) and Pb(II) solution with known initial concentrations of the ternary aqueous solution, the range varying from 10 to 50 mg/l prepared from stock solutions. The adsorbent dosage was 5 g/l. The pH value of each solution was adjusted to remain constant. The flasks were agitated on a shaker at 200 rpm at room temperature. A 1 ml sample was taken from each flask at incremental time intervals. After adsorption, the samples were centrifuged at 16,000 rpm for 10 min and the supernatants analyzed for the residual heavy metal concentration. All experiments were carried out at least twice and the mean values were used in the analysis of data. The amount of metal ions sorbed (q_e) onto CS–MAA nanoparticles was calculated by the following equation

$$q_e = \frac{(C_0 - C_e)V}{W} \quad (1)$$

UNCORRECTED PROOF

where q_e is the equilibrium sorption capacity in mg/g, C_e the final concentration of metal ions in mg/l, V the volume of metal ions solution in l, and W the weight of the adsorbent in grams. The effect of pH on the adsorption of Pb(II), Ni(II) and Cd(II) ions was evaluated by varying the pH from 3 to 5. The adsorption experiments were carried out within the pH range of 3 to 5 due to the fact that metal precipitation appeared at higher pH values and interfered with the accumulation or deterioration of the adsorbent.

The concentration of metal ions adsorbed on the CS–MAA was determined by centrifuging at 16,000 rpm for 10 min to remove the metal ions not adsorbed onto the CS–MAA. The supernatant was diluted in a 10 ml volumetric flask up to mark with distilled water. This solution was injected in to an AA spectrometer (AAS, Philips, PU9400, and UK) with separate calibrations curve for each metal ion. On the other hand, the AA technique requires a calibration curve which was obtained using a standard solution for each metal. In order to reduce the random errors, all experiments were run three times and the average of these measurements is reported. The errors in the adsorption determination of the metal ions were smaller than 0.5%.

2.5. Equilibrium parameters of adsorption

Equilibrium isotherm data obtained from batch experiments were examined using different types of isotherm models such as Langmuir, Freundlich and Redlich–Peterson. The nonlinear form of Langmuir isotherm [26] is given by

$$q_e = \frac{q_m b C_e}{1 + bC_e} \tag{2}$$

where q_e is the equilibrium sorption capacity of sorbent in mg/g, C_e the equilibrium concentration of metal ions in mg/l, q_m the maximum amount of metal sorbed in mg/g and b the constant that refers to the bonding energy of sorption in l/mg. The Freundlich isotherm [27] is express as

$$q_e = K_f C_e^{\frac{1}{n}} \tag{3}$$

where q_e is the equilibrium sorption capacity of the adsorbent in mg/g, C_e the equilibrium concentration of heavy metal ions in mg/l, K_f the constant related to the adsorption capacity of the sorbent in mg/l and n the constants related to the sorption intensity of adsorbent.

The nonlinear form of Redlich–Peterson isotherm [28] is expressed as

$$q_e = \frac{k_{RP} C_e}{1 + \alpha_{RP} C_e^{\beta}} \tag{4}$$

where k_{RP} is the Redlich–Peterson isotherm constant in l/mg, α_{RP} the Redlich–Peterson isotherm constant in $(l/mg)^{\beta}$ and β the exponent that lies between 0 and 1. For if $\beta = 1$, the Redlich–Peterson isotherm becomes a Langmuir isotherm. Nonlinear regression was performed with the statistical software Sigma Plot software for windows (Sigma Plot 10.0, SPSS Inc., USA).

2.6. Adsorption kinetics

In order to evaluate the mechanism of adsorption and the potential steps controlling the rate of adsorption, the basic characteristics of a good adsorbent considering adsorption kinetics under constant temperature and optimum solution pH, were determined, by using various initial metal ion concentrations. The pseudo-first-order and pseudo-second-order kinetic models were applied to the experimental data to predict the adsorption kinetics [29]. The nonlinear form of the pseudo-second-order kinetic model can be written as follows [30]:

$$q_t = \frac{k_2 q_e^2 t}{1 + k_2 q_e t} \tag{5}$$

where k_2 is the adsorption rate constant of pseudo second-order in g/mg min and q_t the adsorption amount at time t in mg/g. The experimental data were further analyzed by using Ho's pseudo-second-order kinetic model [30]

$$\frac{t}{q_t} = \frac{1}{k_2 q_e} + \frac{t}{q_e} \tag{6}$$

The values of k_2 and $q_e{}^2$ of the pseudo-second-order kinetic model can be obtained from the intercept and slope of the plot of t/q_t versus t. The linear regression was performed with the statistical software SigmaPlot software (SigmaPlot 10.0, SPSS Inc., USA) for windows.

2.7. Desorption experiments

The reusability of CS–MAA was investigated in a batch operation. The desorption of adsorbed precious Cd(II), Ni(II) and Pb(II) ions from CS–MAA nanoparticles in NaCl and EDTA solutions was studied. This procedure was used in all the batch desorption experiments using 100 ml of desorption agent in 250 ml Erlenmeyer flasks containing the precious Cd(II), Ni(II) and Pb(II) ions adsorbed onto CS–MAA. In order to get to a state of equilibrium, the flasks were shaken at room temperature at 100 rpm using a mechanical shaker for 3 h at 25 °C. The desorbed precious Cd(II), Ni(II) and Pb(II) ions from CS–MAA were measured by AAS. The Cd(II), Ni(II) and Pb(II) desorbed by the biosorbent were used in the next cycle of adsorption and desorption. The above procedure was employed for three (3) consecutive cycles.

3. Results and discussion

3.1. Characterization of CS–MAA nanoparticles

CS–MAA nanoparticles were prepared by polymerizing methacrylic (MAA) in the presence of chitosan solution [25]. The particles obtained in this manner appeared as white powder and were insoluble in water, dilute acid and alkalescent solutions. The morphology of the CS–MAA nanoparticle (at pH = 4) characterized with SEM image is illustrated in Fig. 1(a)–(c). It can be seen from Fig. 1 that there was a significant difference in the morphology or the shape of the nanoparticles when the CS to MAA weight ratio was in the range of 2:1–1:2. This result suggests that the ratio of CS to MAA may be affected by the morphology and diameter size of the CS–MAA nanoparticles. The ratio of 1:2 w/w of CS to MAA at synthesis and the experimental results showed that the microspheres morphology of CS nanoparticles tend to agglomerates during these experiments, as shown in Fig. 1(a). However, as seen in Fig. 1(b), increasing the weight ratio of CS to MAA causes an increase in both the nanoparticle diameter and the size distribution range, due to the fact that a higher CS to MAA weight ratio leads to the concomitant increase in the particle aggregation and viscosity of the mixture solution. Furthermore, the amine functional groups protonate increasingly at a higher concentration of chitosan, and the repulsive interaction of the positive ions increase the diameter of the nanoparticle. This is because the availability of functional groups on CS and MAA for interaction is in stoichiometric proportion. Thus it is suggested that the best particle size distributions is obtained at an appropriate CS to MAA weight ratio of 2:1, and the SEM morphology is that of the spherical particles, as shown in Fig. 1(c). This indicates that unique diameter and size distribution of the nanoparticles can be

UNCORRECTED PROOF

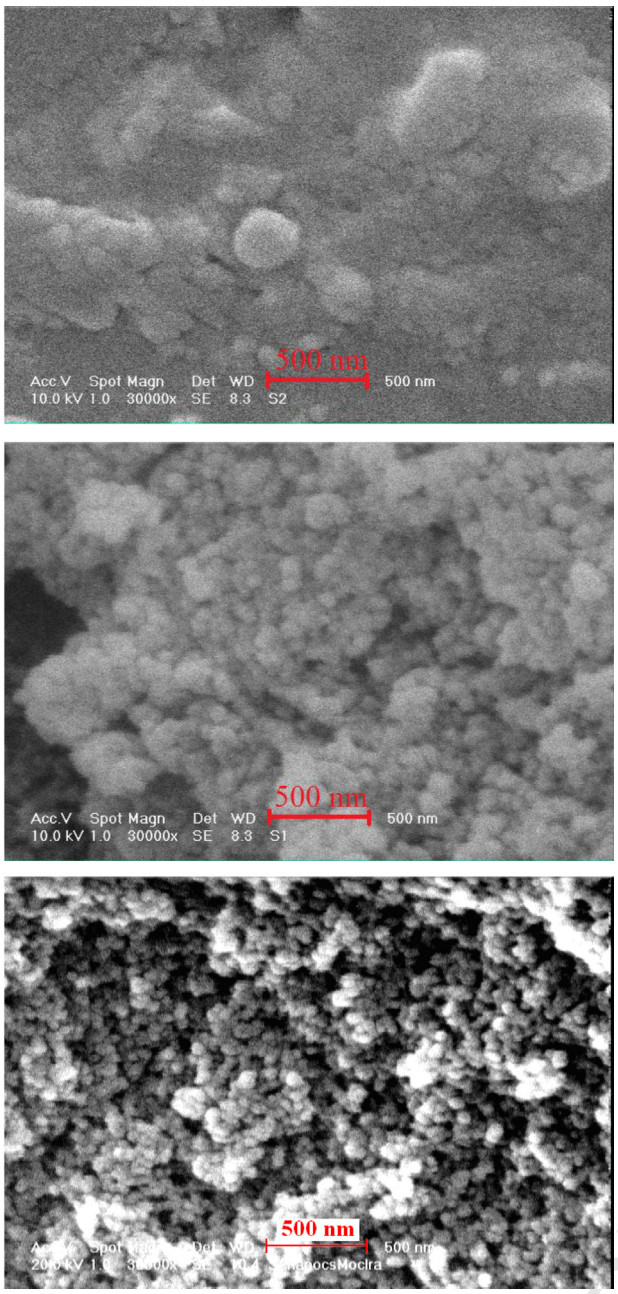

Fig. 1. SEM image of CS–MAA nanoparticles at pH 4 with (a) 1:2, (b) 1:1, and (c) 2:1 weight ratio of chitosan to MAA.

obtained where the optimal CS to MAA is at [COOH]/[NH_2] molar ratio of 4.7:1 (2:1 weight ratio), as shown in Fig. 1(c).

Fig. 2(a) and (b) shows the sizes of the CS–MAA nanoparticle as a function of intensity and nanoparticle size distribution. Increasing the CS–MAA weight ratio causes an increase in the measured mean nanoparticle size, up to 560 nm for the ratios tested as shown in Fig. 2(a). The mean diameter of CS–MAA nanoparticle was obtained at 41 nm, as measured by a zetameter as shown Fig. 2(a). These results suggest that the distribution of the spherical nanoparticles with the smallest diameter can be obtained when the CS to MAA ratio is at 2:1 (w/w, %), as shown in Fig. 2(b). However, with a further increase in the CS to MAA weight ratio up to 1:2, we were not able to measure the particle size distributions because the nanoparticles had a larger size distribution than those with 2:1 and 1:1 ratios, which is difficulty associated with the analysis of particles ≥6000 μm size range, as shown in the morphological SEM image of Fig. 2(c).

Fig. 3 shows the FT-IR spectra of the chitosan (curve a) and CS–MAA nanoparticles (curve b). In Fig. 4(a), the adsorption peaks of chitosan were observed at 3050–3650 cm^{-1} (–OH and –NH_2 stretching), 2924 and 2862 cm^{-1} (–CH stretching), 1581 cm^{-1} (–NH amide band II), 1381 cm^{-1} (–NH amide band III) and 1080 cm^{-1} (–C–O stretching) [31,32]. In Fig. 4(b), the peaks at 1705 and 1544 cm^{-1} are related to (–CONH) functional groups that confirm the presence of MAA in the CS–MAA [33]. Moreover, two peaks at 1550 cm^{-1} and 1643 cm^{-1} are associated with NH_3 and COO^- groups, respectively [34,35]. The absorption around 3000–3600 cm^{-1} (–NH stretching) increases and two new absorption bands appear at 1636 and 1534 cm^{-1}, which originate from the amide band I and amide band II [31].

In Fig. 4 the ^{13}C CPMAS NMR spectra of chitosan and CS–MAA nanoparticles are shown. The chitosan spectrum (Fig. 4(a)) shows signals corresponding to different carbons associated with to the chitosan structure, i.e. 59 ppm (C2, C6), 75.7 ppm (C3), 83.2 ppm (C4) and 105.2 ppm (C1). The signals resonating at 174.3 ppm and 23.9 ppm correspond to the *N*-acetylglucosamine units [36]. In the ^{13}C CPMAS spectrum of CS–MAA (Fig. 4(b)) several new signals are observed. The formation of CS–MAA nanoparticles is implied by the presence of signals at 182.3 ppm (C1), 56.6 ppm (C3), 45.8 ppm (C2) and 18.8 ppm (C4) [37].

XPS analysis is a useful method for specifying the binding energy of carbon (C 1s), oxygen (O 1s) and nitrogen (N 1s) on the surface of adsorbent. XPS high-resolution nitrogen, carbon and oxygen spectra of the chitosan and CS–MAA nanoparticles are shown Fig. 5. As can be seen in Fig. 5, the C 1s spectra of these adsorbents have two peaks with binding energy of 290 and 290.8 eV. Based on the literature, these peaks can be attributed to C=O, O–C–O, and O=C–O bonds of carboxylate groups of CS–MAA nanoparticles [38,39]. Fig. 5 shows two peaks with binding energy of 538 and 537.6 eV in the O1s spectra of chitosan and CS–MAA nanoparticles, respectively. Binding energy peaks can be assigned to C=O in carbonyl, C–O in alcoholic hydroxyl and C–O bond in carboxyl functionalities [40]. There is one peak in the N 1s spectrum at the binding energy of about 400.4 and 398.9 eV for chitosan and CS–MAA nanoparticles, respectively. This is contributed to nitrogen atom in the amine group. The amine group can be protonated under different pH value and made the peak at greater binding energy at 400 eV such as 404.9.

3.2. Effect of pH

The initial pH of the metal solution is one of the most important variables in the adsorption process. The uptake capacity of metal ions and the adsorption mechanism involved are dependent on the pH of the solution, which affects the degree of ionization, the surface charge of the adsorbent and the speciation of the adsorbates [41,42]. This could be attributed to two factors, first, the protonation of amine and carboxylate groups resulting to unavailability of amine and carboxylate groups for complexation with metals, and second, the hydrogen ions (H^+) compete with metal ions for the same binding sites on the adsorbent [22].

At a low pH value of the solution, the carboxylate and amine functional groups in the CS–MAA nanoparticle are protonated to varied degrees and associated with H^+ reducing the number of binding sites available for Pb(II), Ni(II) and Cd(II) ions uptake, reducing the extent their uptake at high concentrations of protons. Moreover, the protonation of amine and carboxylate groups induces an electrostatic repulsion toward Pb(II), Ni(II) and Cd(II) ions. The degree of protonation of the amine groups depends on both the degree of carboxylation and the pK_a of the CS–MAA nanoparticles. When the pH of the solution increases,

UNCORRECTED PROOF

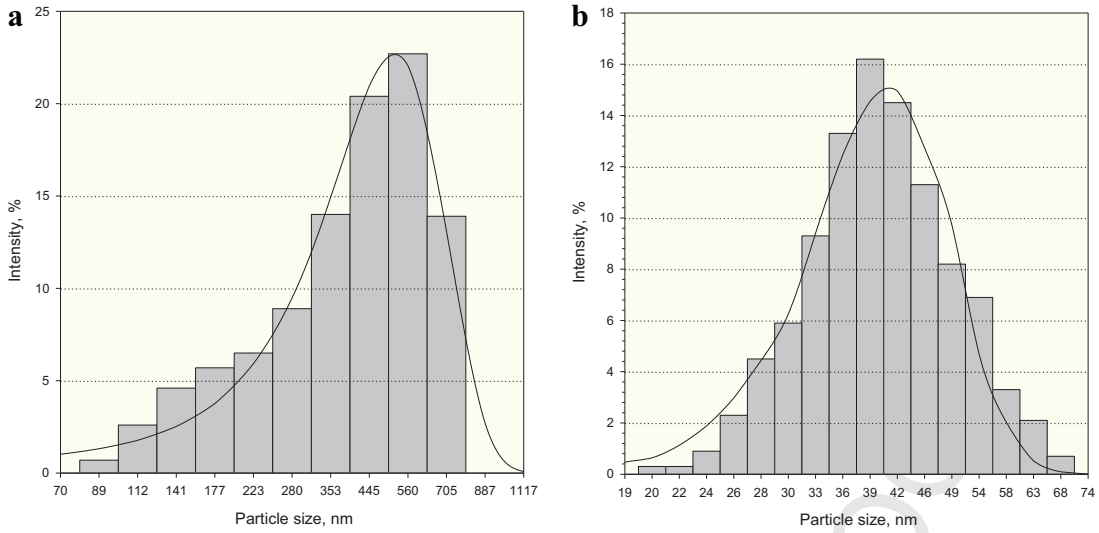

Fig. 2. Size distribution of CS–MAA nanoparticles with (a) 1:1 and (b) 2:1 of CS to MAA ratio.

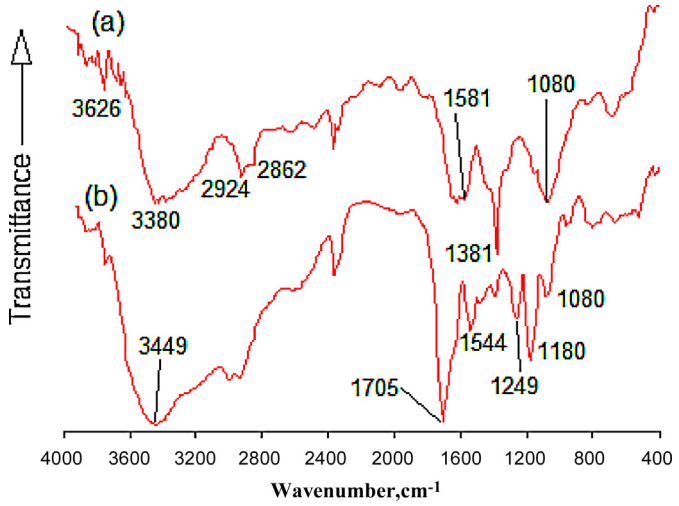

Fig. 3. FT-IR spectra of (a) chitosan and (b) CS–MAA.

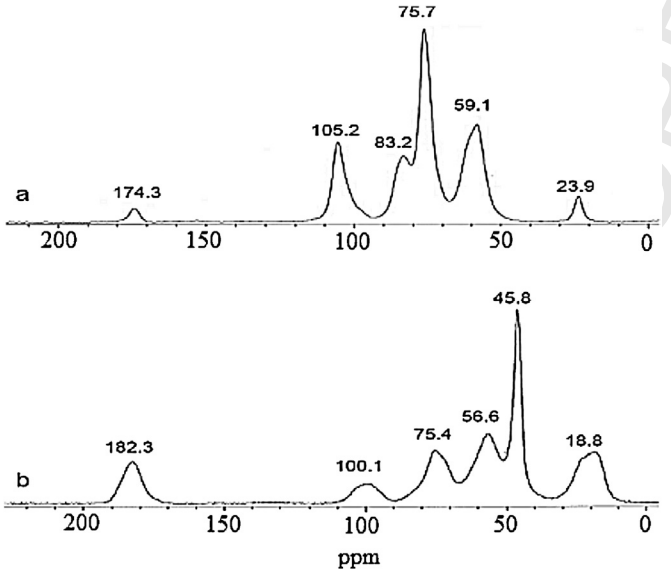

Fig. 4. ^{13}C CPMAS NMR spectra (5 kHz) of (a) chitosan and (b) CS–MAA nanoparticles.

the protonation of the amine group decreases and therefore the electrostatic repulsion decreases [43,44]. As pointed out previously, the pH has also a critical effect on the concentration of metal ions, the charge of the metal species present in the solution and composition of the solution and therefore on their affinity for the adsorbent [23,45]. The pH of the aqueous solution also affects the metal speciation in aqueous solution and the surface properties of the adsorbent. It is observed that at pH less than five (5) the predominant M(II) species is M^{2+} and other species such as $M(OH)^{+}$, $M_2(OH)^{3+}$, $M_3(OH)_4{}^{2+}$ and $M_4(OH)_4{}^{4+}$ are present only in very small amounts. Besides, the surface of the CS–MAA nanoparticle is negatively charged at moderate pH, with a strong electrostatic attraction existing between the surface groups and the M(II) species.

At a high pH, the metal ions react with hydroxide ions to form $Pb(OH)_2$ and $Ni(OH)_2$ compounds, which are solid at room temperature [46]. The experiments with Pb(II) could not be continued beyond pH 6.0 due to the low solubility of Pb(II) hydroxide, an occurrence observed also by other workers [47].On the other hand, at pH less than 5.0 the predominant Pb(II) species is Pb^{2+}, other species such as $Pb(OH)^{+}$, $Pb_2(OH)^{3+}$, $Pb_3(OH)_4{}^{2+}$ and $Pb_4(OH)_4{}^{4+}$ present only in very small amounts [48]. A precipitation of $Ni(OH)_2$

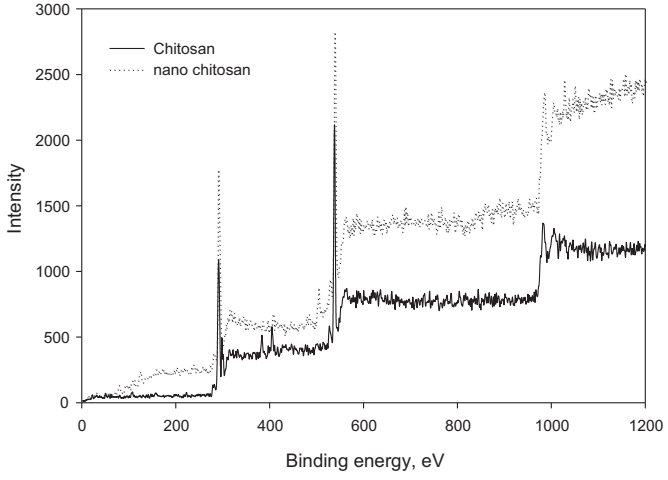

Fig. 5. Representative wide scan of C 1s, O 1s and N 1s XPS spectrum for chitosan and chitosan–MAA nanoparticles.

UNCORRECTED PROOF

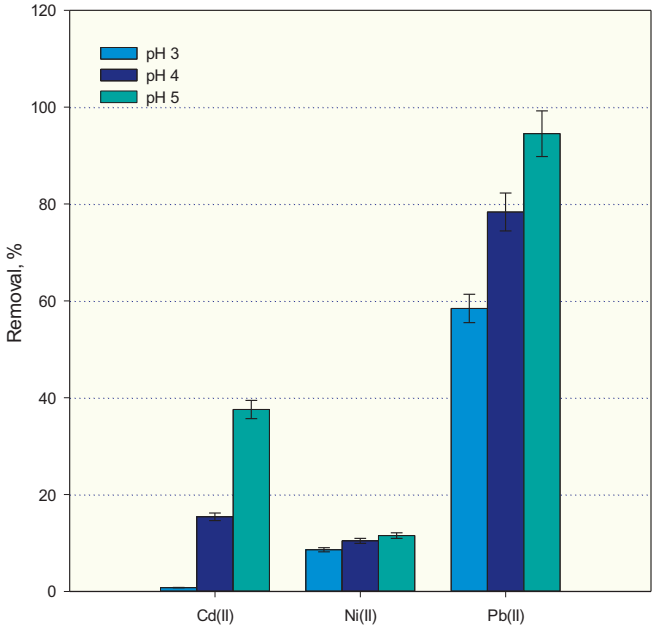

Fig. 6. Effect of pH on adsorption Pb(II),Cd(II) and Ni(II) ions by CS–MAA (dosage 5 g/l, metal concentration of 30 mg/l, contact time of 120 min).

and other species did not occur up to pH 8.0, after which there was no change in the uptake capacity of Ni(II), indicating the precipitation of $Ni(OH)_2$ and related species [47]. Within the pH range studied, the uptake capacity of Cd(II) showed a gradual increase with no indication of precipitation of $Cd(OH)_2$. Cd(II) is mainly found as Cd^{2+} at pH $\leq$8 and from this value up to pH 9 $Cd(OH)^+$ ions may be formed. At pH>9, Cd(II) present in the solution occurs as $Cd(OH)_2$, $Cd(OH)^+$ and $Cd(OH)^{3-}$, and at pH >13 the $Cd(OH)^{3-}$ anions predominate [21]. The decrease in the uptake capacity at higher pH was likely due to the formation of soluble hydroxylated complexes of the metal ions and their competition with the active adsorption sites, as a consequence, the retention would decrease again [49]. At acidic pH, the surface of the adsorbent is positive and may result in a repulsive force between the positively charged surface and the aqueous adsorbate species bearing a similar charge [48]. Fig. 6 demonstrates the effect of pH on the adsorption of Pb(II), Cd(II) and Ni(II) ions by CS–MAA. The percentage of the metal ions adsorption to CS–MAA decreased as the pH of the solution decreased. On the other hand, as the pH of the solution decreases, the amine groups are protonated to varying degrees and the lower extenders of the carboxyl group are dissociated, blocking the interaction of metal ions [50], while the number of binding sites available for chelation with metal ions decreases also [51] and the H^+ ions compete with metal ions for the same binding sites on the adsorbent [22]. The results of the this indicated that the optimum pH for adsorption of Cd(II), Ni(II) and Pb(II) was 5.0. Among the various factors that affect the uptake of metal ions by the adsorbent, the reaction of metal ions with the functional groups on the surface of adsorbents depends largely on the physicochemical properties of metals [52]. It should be noted that the affinity of the CS–MAA nanoparticles was significantly different for the metal ions with different the atomic weights, electronegativity, electrode potential and ionic size of metal ions, so it is clear that electronegativity is an important indicator for adsorption [53]: Thus, the high uptake capacity by CS–MAA of Pb(II) ions resulted from their high atomic weight along with the other related characteristics mentioned above.

3.3. Effect of dose and type of adsorbents

The dose of the adsorbent has a strong influence on the adsorption process. The percent removal of Cd(II), Ni(II) and Pb(II), as function of the adsorbent dose with chitosan and CS–MAA nanoparticles, is shown in Fig. 7(a)–(c). Our experiment was carried out at different doses of adsorbent (5–20 g/l), while the concentration of the metal (50 mg/l at pH 5) and the contact time (120 min) was not changed. The percent removal of Cd(II), Ni(II) and Pb(II) ions increased with increasing the adsorbent dose, which may be due to the increase in the adsorbent surface area and the growing number of available adsorption sites [54].

With an increase in the adsorbent dose, from 5 to 20 g/l, the amount of adsorbed Cd(II), Ni(II) and Pb(II) ions with CS–MAA nanoparticles increased from 20.2% to 72.4%, 8.2% to 15.3% and 90.2% to 97.7%, and with chitosan from 8.2% to 52.8%, 5% to 68.6% and 62.5% to 97.7%, respectively. As Fig. 7 shows, the CS–MAA nanoparticles absorbed Cd(II) and Pb(II) ions in aqueous solution better than chitosan. CS–MAA nanoparticles with the mean size of 30 nm have a higher removal efficiency for Cd(II) and Pb(II) due to different functionalized groups and a variable distribution of carboxyl groups in comparison with chitosan and also compared to the decrease in the time required to reach equilibrium. The sorption performance of chitosan and its derivatives can be significantly affected by the particle size and the conditioning of the sorbent due to the diffusion restrictions caused by the low porosity and crystallinity of the raw chitosan [55]. Most studies have shown that CS–MAA nanoparticles are superior in enhancing the metal ions adsorption from aqueous solution as compared to chitosan. On the other hand, the use of CS–MAA nanoparticles as adsorbent for Cd(II), Ni(II) and Pb(II) adsorption from aqueous solution seems beneficial due to its high amino and carboxyl functional groups. This could be because a functionalized particle may preferentially improve the level of reactivity by a fast diffusion (i.e. enhanced kinetics) onto the CS–MAA cross-linked nanoparticle. However, one of the key benefits identified for CS–MAA nanoparticles in comparison to zeolite has been the rapid adsorption of Cd(II), Ni(II) and Pb(II) from aqueous solution [56] and the activated carbon [10] which both require a somewhat higher contact time.

The removal efficiency is not significantly increased with an increase in the adsorbent dose. Evidently, the optimum amount of CS–MAA nanoparticles for further adsorption experiments with 5 g/l and the removal of Cd(II), Ni(II) and Pb(II) were found to be 20.2%, 15.3% and 90.2%, respectively. In addition, the removal efficiency of metal ions decreased from 5 to 20 g/l with the increase in the adsorbent dosage (Fig. 7). It is to be noticed that the both a different equilibrium concentration and adsorption capacity was reached when various adsorbent dosages were used. The maximum uptake capacity at 5 g/l of CS–MAA nanoparticles was determined as 1.84 mg Cd(II)/g, 0.87 mg Ni(II)/g and 11.3 mg Pb(II)/g. The affinity of chitosan to transition metal cations depends on parameters such as the total number of free amine groups (deacetylation degree), the number of available free amine groups and diffusion properties [57,58]. It should be noted that hard acids bind preferentially to oxygen donor ligands (hard) such as the carboxylate groups in CS–MAA, while soft acids bind preferentially to ligands containing nitrogen or sulphur (soft) such as the amine groups in chitosan [59]. The decrease in the adsorption of Ni(II) by CS–MAA comparing to that by chitosan may be related to a lower amine group in its structure: this again is because of the grafting of carboxyl functional groups on CS–MAA nanoparticles for preparing an adsorbent for both soft and hard acids. Moreover, by decreasing the particle size of the adsorbent, the external and intra-particle diffusion coefficients are decreased, causing a decrease in the adsorption of Ni(II) by CS–MAA [43].

UNCORRECTED PROOF

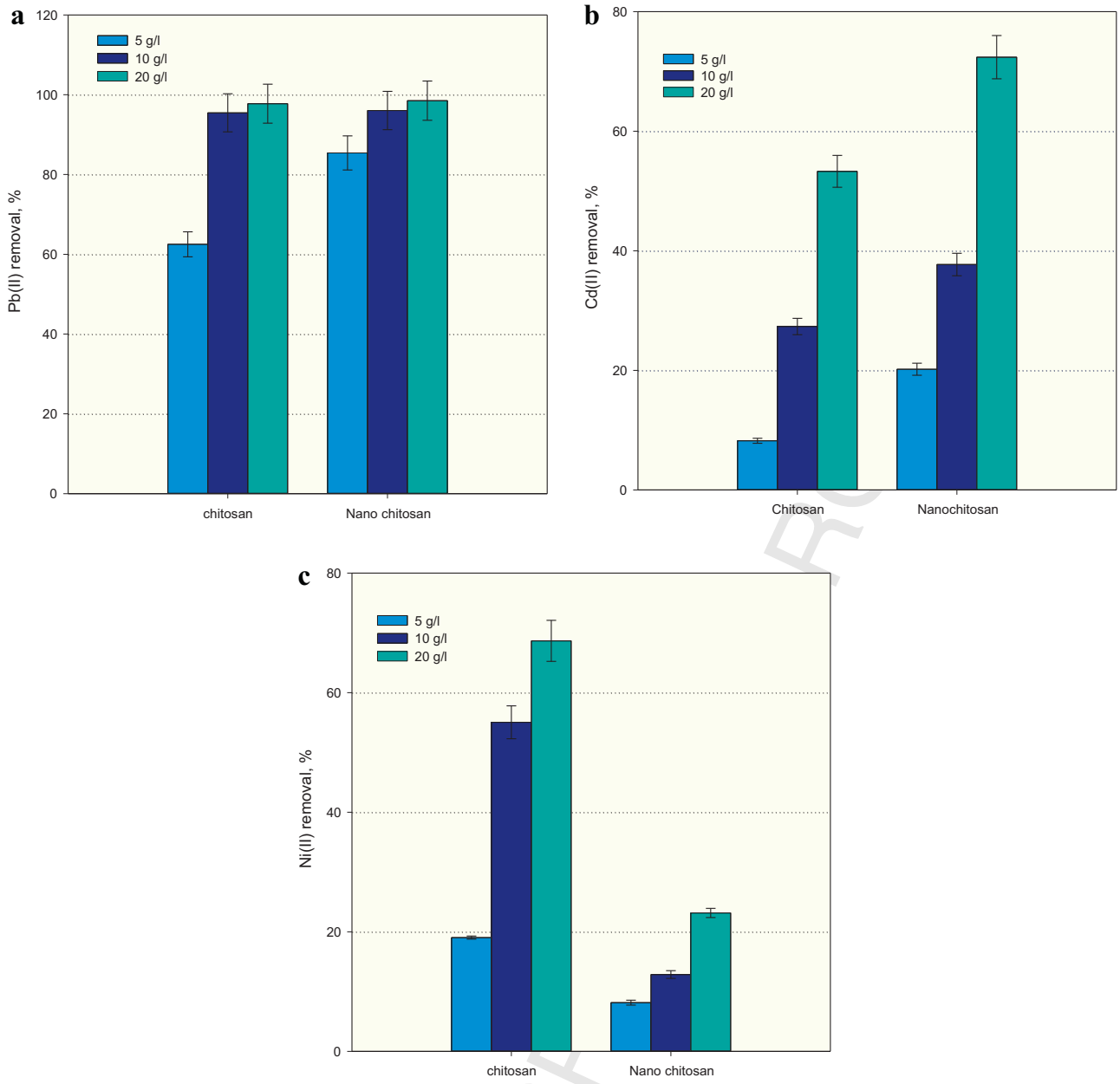

Fig. 7. Effect of dosage on adsorption (a) Pb(II), (b) Ni(II) and (c) Cd(II) ions by CS–MAA nanoparticle and chitosan (pH 5, metal concentration of 50 mg/l, contact time of 120 min).

This result suggests that a large adsorbent dosage reduces the unsaturation of the adsorption sites and likewise the number of such sites per unit mass decreases, resulting a relatively much reduced adsorption at a higher adsorbent dosage [60,61]. In the natural form of the chitosan biopolymer which is in the bulk the available sites on the surface of chitosan are limited for the adsorption of heavy metal ions. However, introducing new functional groups ($-COO^-$) on the surface of chitosan by means of MAA when CS–MAA nanoparticles are formed, resulting in an increase of available sites. There are several reasons for introducing new functional groups (both amine and carboxylic) on the surface of chitosan such as to increase the density of sorption sites, to change the pH range for metal sorption and to vary the sorption sites and/or the uptake mechanism, in order to increase sorption selectivity for the target metal [58].

3.4. Adsorption isotherms

The Langmuir, Freundlich and Redlish–Peterson isotherms were applied to describe the equilibrium data. The Langmuir model assumes that the maximum adsorption takes place in a monolayer of the adsorbate molecules on the adsorbent surface and that all adsorption sites have equivalent energy and negligible interaction between adsorbed molecules [62]. The Freundlich adsorption isotherm, however, is an empirical model and can be used in the case of a heterogeneous surface energy system [5,63]. Furthermore, the Redlich–Peterson model incorporates three parameters into an empirical isotherm and, therefore, can be applied either in homogenous or heterogeneous systems due to its high versatility [64]. Thus, the Cd(II), Ni(II) and Pb(II) equilibrium data on CS–MAA nanoparticles from the isotherm studies were fitted to Langmuir,

Table 1
Langmuir and Frendlich parameters for Cd(II), Ni(II) and Pb(II) ions using CS–MAA.

Metals	Langmuir			Freundlich			Redlich–Peterson			
	q_m (mg/g)	b (l/mg)	R^2	K_f (mg/g)(mg/l)$^{-n}$	n	R^2	k_{RP} (l/mg)	a_{RP} (l/mg)	β	R^2
Cd(II)	2.42	0.25	0.9924	0.86	3.70	0.9962	1.67	1.44	0.81	0.9986
Ni(II)	1.13	0.11	0.9872	0.30	3.31	0.9902	2.38	7.56	0.71	0.9904
Pb(II)	13.72	0.52	0.9675	4.64	2.20	0.9846	32.47	5.90	0.61	0.9857

Table 2
The physicochemical of Cd(II), Ni(II) and Pb(II) ions.

Metal ions	Ionic radius (pm)	Electronegativity	Atomic weight	Characteristics
Pb(II)	133	2.1	207.2	Borderline
Cd(II)	109	1.69	112.41	Soft
Ni(II)	83	1.91	58.71	Borderline

Freundlich and Redlich–Peterson adsorption isotherm models as shown in Fig. 8. The adsorption parameters calculated for the adsorption of Cd(II), Ni(II) and Pb(II) on CS–MAA nanoparticles are summarized in Table 1. The model parameters for the adsorption of Cd(II), Ni(II) and Pb(II) on CS-MAA nanoparticles were statistically significant at 95% confidence levels for Langmuir (correlation coefficient, $0.9675 < R^2 < 0.9924$), Freundlich ($0.9846 < R^2 < 0.9962$) and Redlich–Peterson ($0.9857 < R^2 < 0.9986$) isotherm models. The Redlich–Peterson and Freundlich isotherm models predicted the adsorption data to CS-MAA nanoparticles better than did the Langmuir model, because the high correlation coefficients ($R^2 > 0.99$) were obtained at a higher confidence level. The constant value β of the Redlich–Peterson isotherm model was 0.81, 0.71 and 0.61 for Cd(II), Ni(II) and Pb(II), respectively, which was lower than unity, indicating that the heterogeneous adsorption of Cd(II), Ni(II) and Pb(II) onto CS-MAA nanoparticles was predominant. On the other hand, Redlich–Peterson coefficient, β, remained less than unity indicating the process to have conformed to the experimental Freundlich model, of adsorption onto a heterogeneous surface. Although the correlation coefficients were obtained according to the Langmuir and Freundlich models for Pb(II), Ni(II) and Cd(II) ions, and they both were close. The judgment as to which mechanism is operative is usually based on the correlation coefficient, which is sometimes better for Langmuir and for Freundlich isotherm at other times. For example, Ng et al. studied the sorption of lead ions from aqueous solution onto chitosan and showed that between the three, the Freundlich equation is the best fit equilibrium data based on a linearized correlation coefficient [65]. On the other hand, Popuri et al. showed that both models predicted adequately the experimental data for the adsorption of Ni(II) by chitosan coated PVC beads [14]. The interactions of metals with chitosan are complex and may involve various mechanisms (chelation, ion exchange, electrostatic attraction, etc.) which probably simultaneously dominate by adsorption, ion exchange and chelation [66].

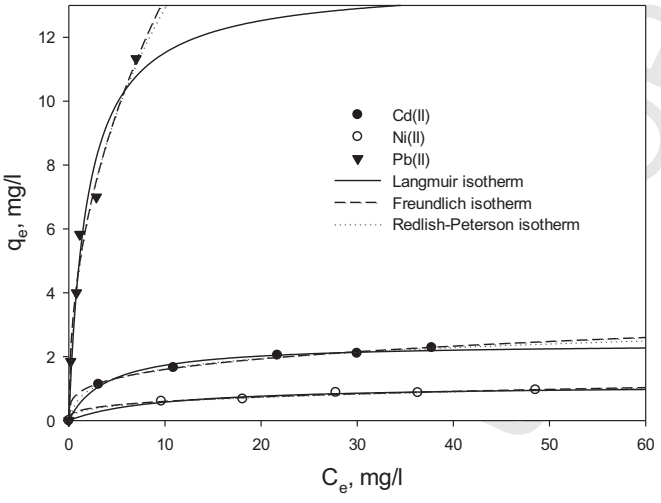

Fig. 8. Langmuir, Freundlich and Redlich-Peterson isotherm models for the adsorption of Cd(II), Ni(II) and Pb(II) by CS–MAA (dosage 5 g/l, pH 5, contact time of 120 min).

The Freundlich constants K_F and $1/n$ for Pb(II) were found to be 2.25 mg/g and 1.19, respectively (Table 1). The values of $1/n$ are less than 1 for all three metal ions, indicative of the degree of nonlinearity between the solution concentration and amount of metal ions adsorbed. However, high the K_F indicated that the Pb(II) adsorption capacity of CS–MAA nanoparticles was high; the low $1/n$ suggested that any large change in the equilibrium concentration of Pb(II) ions would not result in a change in the amount of Pb(II) sorbed by the CS–MAA nanoparticles. According to the values of the correlation coefficient (R^2), the best-fit isotherm model was the Redlich–Peterson one. The conclusion is that the Redlich–Peterson isotherm model supported the Freundlich isotherm model. This result can be also confirmed from the value of the β in Table 1, which is lower than unity (<1) [64,67].

Nevertheless, there are many studies in the literature indicating that the adsorption mechanism of metal ions is described by different experimental models, depending on the metal species and types of chitosan particles [68]. For the case of Pb(II), Cd(II) and Ni(II) ions, the equilibrium isotherms in other studies are best represented by the Langmuir model. The maximum adsorption capacity values (q_m) for Pb(II), Cd(II) and Ni(II) ions were 13.72, 2.42, and 1.13 mg/g, respectively, which indicates selectivity of CS–MAA for the adsorption of metal ions. The increase in the maximum adsorption capacity of the CS–MAA nanoparticles was observed in the following order: Pb(II) > Cd(II) > Ni(II). The high adsorption affinity we found for Pb(II) which may be linked to the physicochemical properties of Pb(II) (Table 2).

The relative selectivity of heavy metals is, in general, related to some relevant metallic properties. The affinity sequences for their adsorption increases based on the ionic radii, atomic weight, electronegativity, hydrolysis constant, and softness of the metal [53]. On the other hand, the interaction between the heavy metal ions and the NH_2 groups (as binding sites) depends on hard and soft acids and bases (HSAB) besides the charge and size of the metal ions. Pb(II) is considered a soft heavy metal (class B), while Ni(II) and Cd(II) are considered a borderline case between hard (class A) and soft (class B) metals [53]. Nevertheless, the amine groups of chitosan, when responsive to Cd(II) ions they are known as soft base ligands, then the interaction between this ligand and the soft Lewis acids (metal ions) is easier. However, borderline metal ions could bind soft and hard base ligands with different preferences. Therefore, the presence of ligands and this type of metal ions strongly controls the adsorption isotherm and the uptake capacity

UNCORRECTED PROOF

Table 3
Comparison of maximum adsorption capacities of Cd(II), Ni(II) and Pb(II) on chitosan adsorbents in single and multi element system.

Metal	System	Adsorbent	pH	Contact time	Particle size	q_e (mg/g)	Refs.
Pb(II)	Single-component	Chitosan nanofibers	4.6	24 h	235 nm	263.15	[79]
		Chitosan nanoparticles	5.5	24 h	40 nm	398.00	[23]
		Chitosan	5	24 h	300–425 μm	141.10	[46]
			4.5	336 h	303 μm	1.37	[65]
			4.5	336 h	605 μm	0.23	[65]
			5	24 h	300–425 μm	141.10	[46]
	Multi-metal component	Chitosan	4	–	–	3.33	[21]
Cd(II)	Single-component	CS–MAA	5	120 min	20–68 nm	11.30	This study
		Chitosan	8	504 h	–	105.00	[80]
	Multi-metal component		7	24 h	–	150.00	[43]
			4	–	–	5.32	[21]
Ni(II)	Single-component	CS–MAA	5	120 min	20–68 nm	1.84	This study
		Chitosan	5	24 h	300–425 μm	52.86	[46]
	Multi-metal component	Chitosan	5	–	–	2.40	[11]
		CS–MAA	5	120 min	20–68 nm	0.87	This study

mechanism. Thus selectivity can be enhanced by a chemical modification of the adsorbent surface by introducing new functional groups. This study elucidates the fact that the difference in the ionic size is not the only dominant factor in the adsorption process metals ions, meaning that the adsorption process may be affected by the density of the ion charge and/or by the orbital energy valence, which is a measure of the strength of the covalent bonding relative to ionic bonding. In this study, the uptake capacity of the CS–MAA for Pb(II) was found to be higher than that for Ni(II). In the case of chitosan, the metals Ni(II), Cd(II) and Pb(II) with empty orbitals function as a Lewis acid capable of accepting electron pairs. This means that the NH_2 functional groups that have nonbonding electron pairs function as Lewis bases donating their electrons pair [21]. The maximum adsorption capacities for Ni(II), Cd(II) and Pb(II) on chitosan and CS–MAA in a single metal solution are reported in Table 3 [23,53]. The simultaneous presence of Cd(II), Pb(II) and Ni(II) in an aqueous solution leads to a low adsorption capacity, which changes the maximum uptake (q_m) for each component [1]. The metal ions at maximum are competing for the same binding sites [53]. Moreover, the maximum adsorption capacity increased with an increase in the contact time and an equilibrium was established in the first 5 min of the contact time. After an equilibrium time at 120 min, no more Cd(II), Ni(II) and Pb(II) were adsorbed. The equilibrium adsorption time in this study was much shorter than what has been previously reported in literature (Table 3).

It is the adsorption mechanisms and reaction process between the metal ions and the functional groups on the adsorbent surface that are of interest. The mechanism responsible for the adsorption of heavy metals is a physicochemical process and may be one or a combination of many ion exchanges, or surface complexation, coordination, adsorption, absorption, electrostatic interaction, chelation and microprecipitation. The adsorption of Ni(II) onto CS–MAA was decreased by 53.3%, which can be said to be because, due to a cross-linked polymerization, a portion of the amine groups present in chitosan involved in Ni(II) adsorption will be excluded. Since the percent removal of Cd(II) and Pb(II) was increased by 12% and 27.7%, respectively, it suggests that the most important metal binding groups are represented by the carboxyl ones, due to a condition where highly negatively charged CS–MAA nanoparticles can serve as an adsorption mechanism. Therefore, the percentage of the removal of Cd(II), Ni(II) and Pb(II) ions from aqueous solutions is strongly influenced by the surface morphology of the adsorbent. The results also show that the mechanism of the adsorption is heterogeneous adsorption. This conforms with the assumption that it is the different types of the functional groups that are mainly responsible for heavy metal binding and adsorption, on other words, the surface complexation may be the main mechanism of the adsorption of heavy metals.

3.5. Adsorption edge in aqueous system

The removal of Cd(II), Ni(II) and Pb(II) ions, ranging from 10 to 50 mg/l by the optimum dose of 5 g/l of CS–MAA nanoparticles at pH 5, was studied by conducting batch experiments at room temperature. The amount of Pb(II) adsorbed on the surface of CS–MAA was significantly higher than of Cd(II) and Ni(II), which indicates that the functional group (namely, carboxylic) which is dissociated on the surface of CS–MAA nanoparticles, promotes Pb(II) removal. We observed that the carboxylic and amine groups are the main adsorption sites on this adsorbent. However, the weak adsorption capacity for Cd(II) and Ni(II) ions indicates that the carboxylic group is the major functional group responsible for the Pb(II) removal by this adsorbent. In order to indicate a more reliable description of this fact, the decrease in the adsorption capacity of Cd(II) and Ni(II) in the presence of Pb(II) could be attributed to the difference in their class behavior on the basis of their covalent indices, which indicates a competitive effect. It should be mentioned that Pb(II) is classified as a class B ion, while Cd(II) and Ni(II) are classified as class A ions.

The comparison of the adsorption capacity of the CS–MAA nanoparticles used in this study with results obtained according to the literature proves consistently that CS–MAA is effective for enhancing adsorption. Qi and Xu [23] used CS–MAA nanoparticles (between 40 and 100 nm) for sorption of Pb(II) ions from aqueous solution with the maximum uptake capacity of Pb(II) ions was obtained at the pH 5.5. The highest amount of adsorbed at 60 and 900 mg/l Pb(II) ions concentration on CS-MAA nanoparticles was found to be 48 and 398 mg/g, respectively, and the corresponding removal efficiency was 80% and 38.9%, respectively. Haider and Park [24] studied Cu(II) and Pb(II) ions removal from aqueous solution in the single-ion situation with chitosan nanofibers materials. They reported that the chitosan nanofibers materials adsorbed Pb(II) with the adsorption capacity of 263.15 mg/g at pH 5.0. when Paulino et al. [46] removed Pb(II) and Ni(II) using chitosan produced from silkworm chrysalides (75% deacetylation degree), the adsorption capacities of Pb(II) and Ni(II) onto chitosan were found to be 141.10 and 52.81 mg/g, respectively, at pH 5 and contact time of 24 h. They reported that the chitosan showed notable binding affinity for Pb(II) but it adsorbed Ni(II) less efficiently. Ng et al. [65] investigated the adsorption of Pb(II) ions on chitosan and observed that the adsorption capacity of the chitosan for Pb(II) was 115.5 mg/g at pH 4.5 with contact time of 14 days and the corresponding removal efficiency was 81.4%. In another study, in order to determine the selectivity of chitosan, the adsorption capacities of Pb(II) and Ni(II) onto chitosan were investigated. They reported the amounts of adsorbed Pb(II), Cd(II) and Cu(II) at 100 mg/l on the chitosan at pH 4.0 to be 7.45, 1.80 and 0.66 mg/g, respectively [21]. In our study, obviously

UNCORRECTED PROOF

Table 4
Pseudo-second-order parameters for adsorption of Cd(II), Ni(II) and Pb(II) ions onto CS–MAA.

Metal ions	Concentration (mg/l)	q_e (mg/g)	k_2 (g/mg min)	R^2
Cd(II)	10	1.53	0.069	0.9987
	20	1.92	0.098	0.9975
	30	2.70	0.106	0.9984
	40	3.30	0.074	0.9942
	50	3.94	0.070	0.9933
Ni(II)	10	0.71	0.049	0.9929
	20	0.80	0.052	0.9916
	30	0.88	0.052	0.9916
	40	1.03	0.042	0.9969
	50	1.12	0.055	0.9950
Pb(II)	10	1.86	0.285	0.9999
	20	4.05	0.590	0.9999
	30	6.51	0.431	0.9958
	40	8.03	0.780	0.9998
	50	11.52	0.492	0.9997

that the adsorption capacities of the Cd(II), Ni(II) and Pb(II) ions on CS–MAA nanoparticles found at 11.30, 1.84, and 0.87 mg/g, respectively, were lower than the values found for chitosan and modified chitosan in literature, however, the fast uptake rate and the adsorption equilibrium time of CS–MAA was much shorter (120 min) than that for chitosan and modified CS–MAA nanoparticles (24 h). Therefore, the corresponding removal efficiency of the Cd(II), Ni(II) and Pb(II) ions was 20.2%, 15.3% and 90.2%, respectively, at pH 5.0 and initial ions concentration of 50 mg/l in ternary aqueous solution. On the other hand, the CS–MAA nanoparticles as adsorbent were found to be most effective in removing the toxic Pb(II) ions from an aqueous solution.

3.6. Kinetics of adsorption

Elucidation of the kinetic parameters and adsorption characteristics of the adsorbent materials is necessary in order to apply the adsorption technique to larger scale processes [53] because kinetic modeling not only shows estimation of adsorption rates but also leads to how to express suitable rates that are characteristic of possible reaction mechanisms [53]. The pseudo-second-order kinetic model is based on the assumptions that the chemical sorption is the rate-limiting step and that mass transfer in solution is not involved [53,69]. This means that there is an external surface mass transfer process that controls the early stage of the adsorption process [70]. On the other hand, the sharp rise in the early stages of the adsorption process is also considered to be indicative of a fast initial mass transfer step [71].

The adsorption kinetics of Cd(II), Ni(II) and Pb(II) using the pseudo-second-order kinetic model with various initial concentrations of heavy metal ions were estimated (Fig. 9).

The kinetics curve for Cd(II), Ni(II) and Pb(II) confirmed that the adsorption was rapid for the first 30 min and then slowed down considerably. On the other hand, the experimental data suggest that the adsorption capacity increased with increasing contact time and reached an equilibrium at 120 min. Therefore, in the present study, we selected 120 min contact time for the equilibrium data calculations. Thus, the difference in contact time of CS–MAA nanoparticles obtained from our kinetics study for Cd(II), Ni(II) and Pb(II) ions is considerable and the contact time was found to be the lowest among those for the corresponding chitosan adsorbents reported in the literature (Table 4).

The values of q_e, and k_2 of fitting experimental data with pseudo-second-order models are summarized in Table 4. The good linearized plots of t/q_t vs. t according to Eq. (6) indicate the validity of the pseudo-second-order kinetic model. We observed that the value of R^2 for pseudo-second-order kinetic model was higher for all three metal ions, which indicated that the pseudo-second-order kinetic model is the best one in describing the adsorption kinetics of metal ions on CS–MAA nanoparticles. We also observed that the Pb(II) was fitted better than Ni(II) or Cd(II) with this model, with the correlation coefficient $R^2 = 0.9999$. Linear correlation coefficients higher than 0.99 indicate the applicability of the pseudo-second order model for the adsorption process of metal ions on CS-MAA nanoparticles. It is also apparent from Table 4, that the rate constant (k_2) of Pb(II) for all of concentrations is higher than that of Cd(II) and Ni(II) indicating a high affinity between Pb(II) ions and the CS–MAA nanoparticles. It is shown in Table 4 that for all Cd(II), Ni(II) and Pb(II) the adsorption onto CS–MAA nanoparticles was rapid at first, which this fact may be explained by the availability of different and more active sites on nanoparticle adsorbents, while the faster adsorption rate of Pb(II) compared to Cd(II) and Ni(II) suggests that $-COO^-$ groups were readily available and easily accessible, the uniform CS–MAA nanoparticles probably facilitating the Pb(II) transfer in the adsorption process. The equilibrium adsorption capacity of Pb(II) onto CS–MAA nanoparticles reached within 120 min, with initial concentrations of 10, 20, 30, 40 and 50 mg/l was 1.86, 4.13, 6.51, 8.03 and 11.52 mg/g, respectively. In parallel, the values of the rate constant, k_2, were recorded at 0.285, 0.590, 0.431, 0.780 and 0.492 g/mg min.

Further, the results in Table 4 show that the uptake rates of the divalent Cd(II) and Ni(II) ions were inhibited by Pb(II) ions because of their larger ionic radii and electronegativity (Table 2) [70,71]. This demonstrates that the competing adsorptive ions have no effect on the adsorption of Pb(II) on CS–MAA nanoparticles.

Overall, the adsorption process can be described as follows, as these results suggest: The pseudo-second-order kinetic model is predominant and that chemisorption may be the rate-limiting step that controls the adsorption process. The Pb(II) is selectively adsorbed on the surface of CS–MAA nanoparticles where physicochemical interactions arise leading to competitive adsorption on the CS–MAA nanoparticles. The metal ions adsorption of CS–MAA nanoparticles depends mainly on the ionic nature of binding, especially soft ions show a more covalent degree [72]. This is in agreement with previous studies on the adsorption of Pb(II), i.e. onto *Ceramium virgatum* [73], *Cladonia furcata* [49], *Saccharomyces cerevisiae* [74] and *Aspergillus niger* [75,76]. Therefore, these results do show that the development of selective metal-binding nanoparticles and highly selective bioengineered adsorbents indicates suggests a promising research direction for industrial application. The United States environmental protection agency (USEPA) has proposed effluent standards for metals in industry. The proposed standards on Ni(II), Cd(II) and Pb(II) are 1.1, 0.7 and 0.1 mg/l, respectively [77]. The adsorption performance of CS–MAA nanoparticles for Pb(II) from artificial wastewater at optimum pH (5) and dosage (5 g/l) and 10–40 mg/l metal concentration greatly meets USEPA

UNCORRECTED PROOF

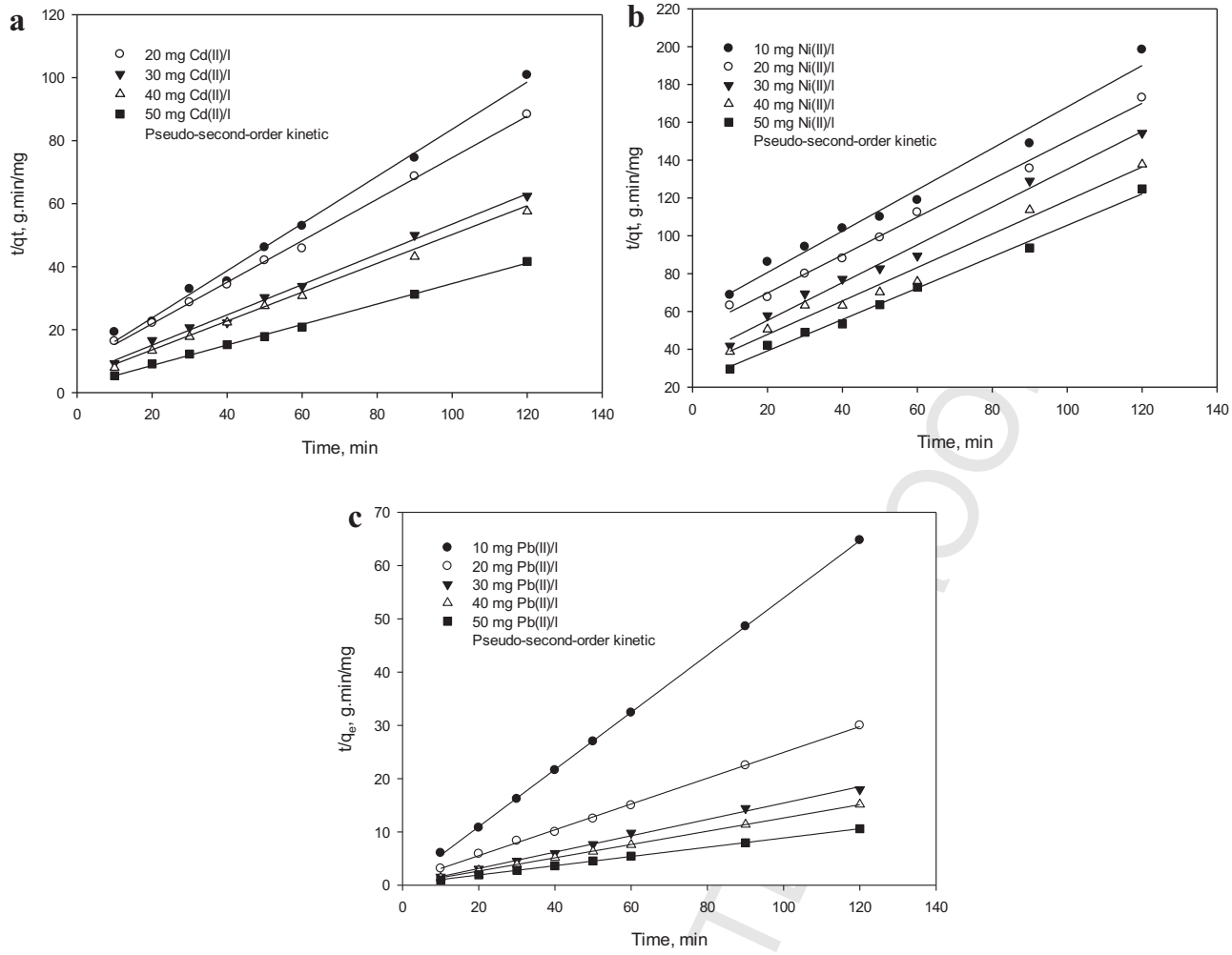

Fig. 9. Pseudo-second-order plots for adsorption (a) Cd(II), (b) Ni (c) Pb(II) ion by CS–MAA nanoparticle (pH 5, dosage 5 g/l, contact time of 120 min).

standard while Ni(II) and Cd(II) concentrations in the effluent were higher than the USEPA standards which are absolutely because of the selectivity of CS–MAA nanoparticles for Pb(II).

3.7. Desorption and regeneration

Desorption from CS–MAA nanoparticles with previously adsorbed Ni(II), Cd(II) and Pb(II) ions was conducted in 100 ml of batches working solutions of 1 M NaCl and 0.1 M EDTA. When agitated for 3 h at room temperature. It was found that NaCl desorbed Cd(II) and Ni(II) better than EDTA, whereas Pb(II) was completely desorbed by EDTA. These control results demonstrate that the amount of adsorption of Ni(II), Cd(II) and Pb(II) ions on CS–MAA nanoparticles did not change significantly with up to three recyclings, as the adsorption recovery was above 95%. There are two basic mechanisms for the adsorption of metal ions by chitosan, namely, electrostatic interactions or van der Waals force (physisorption) and covalent bonds (chemisorption: chelation and ion exchange) which may happen simultaneously [21,78]. It is well known that EDTA is a strong chelating agent. If a solution of EDTA can desorb the metal ions from the sorbent, it is believed that chelation may explain the desorption [58]. The complexation of the metal ions by the ligand did not displace the metal significantly from the sorbent. The desorption of Pb(II), Cd(II) and Ni(II) ions using NaCl may be explained by an electrostatic interaction between metal ions and the charged species from elution, through the compression of the electric double layer, which would weaken the interaction between chitosan and metal [78]. Therefore, NaCl desorbed Cd(II) and Ni(II) from CS–MAA better than EDTA probably due to the fact that in desorption the mechanism of electrostatic interaction is more effective than chelation.

4. Conclusions

These experiments on the ability of CS–MAA nanoparticles to remove Cd(II), Ni(II) and Pb(II) from aqueous solution were conducted as function of the pH, adsorbent dose and initial metal ions concentration. CS–MAA nanoparticles were produced by polymerizing MAA in chitosan (CS) solution. The morphology and the composition of the biosorbent were characterized by using SEM images, NMR spectroscopy, and Zetasizer analyzer and FT-IR spectra. Our experiments showed that the presence of amine and carboxylic groups in the CS–MAA nanoparticle composition provided binding sites for the metal ions. The Langmuir adsorption and Freundlich models were used for analyzing the efficiency of adsorption of Cd(II), Pb(II) and Ni(II) ions onto CS–MAA nanoparticles. The adsorption isotherm was better explained by the Freundlich rather than by the Langmuir model. The maximum adsorption capacity was 11.30, 1.84 and 0.87 mg/g for Pb(II), Cd(II) and Ni(II) ions, respectively, obtained by the Langmuir model. The pseudo-second-order kinetic model was fitted with the adsorption data of Pb(II), Cd(II) and Ni(II) ions onto CS–MAA nanoparticles at various metal concentrations. For CS–MAA nanoparticles and for the three metal

UNCORRECTED PROOF

ions studied, the value of the adsorption capacity increased in the following order: Pb(II) > Cd(II) > Ni(II). The aforementioned results suggest that the nanoparticles, developed as a natural biopolymer-based biodegradable packaging material, can be used selectively for the elimination of heavy metal pollution from wastewater. Therefore, the CS–MAA nanoparticles could be successfully applied as adsorbent for the recovery of Ni(II), Cd(II) and Pb(II) ions from water and wastewater.

Acknowledgments

This work was supported by the Tarbiat Modares University (TMU) of Iran. The authors wish to thank Mrs. Haghdoust for her invaluable technical assistance (Technical Assistant of Environmental Laboratory) and Ellen Vuosalo Tavakoli (University of Mazandaran) for final editing of the English text.

References

[1] S.K. Papageorgiou, F.K. Katsaros, E.P. Kouvelos, N.K. Kanellopoulos, Prediction of binary adsorption isotherms of Cu^{2+}, Cd^{2+} and Pb^{2+} on calcium alginate beads from single adsorption data, J. Hazard. Mater. 162 (2009) 1347–1354.
[2] T. Gotoh, K. Matsushima, K.-I. Kikuchi, Adsorption of Cu and Mn on covalently cross-linked alginate gel beads, Chemosphere 55 (2004) 57–64.
[3] O.M.M. Freitas, R.J.E. Martins, C.M. Delerue-Matos, R.A.R. Boaventura, Removal of Cd(II), Zn(II) and Pb(II) from aqueous solutions by brown marine macro algae: Kinetic modelling, J. Hazard. Mater. 153 (2008) 493–501.
[4] A. Heidari, H. Younesi, Z. Mehraban, Removal of Ni(II), Cd(II), and Pb(II) from a ternary aqueous solution by amino functionalized mesoporous and nano mesoporous silica, Chem. Eng. J. 153 (2009) 70–79.
[5] A.T. Paulino, L.B. Santos, J. Nozaki, Removal of Pb^{2+}, Cu^{2+}, and Fe^{3+} from battery manufacture wastewater by chitosan produced from silkworm chrysalides as a low-cost adsorbent, React. Funct. Polym. 68 (2008) 634–642.
[6] A. Sari, D. Mendil, M. Tuzen, M. Soylak, Biosorption of Cd(II) and Cr(III) from aqueous solution by moss (*Hylocomium splendens*) biomass: equilibrium, kinetic and thermodynamic studies, Chem. Eng. J. 144 (2008) 1–9.
[7] S. Hajialigol, M.A. Taher, Taher, A. Malekpour, Malekpour, A new method for the selective removal of cadmium and zinc ions from aqueous solution by modified clinoptilolite, Adsorpt. Sci. Technol. 24 (2006) 487–496.
[8] M. Soylak, A. Kars, I. Narin, Coprecipitation of Ni^{2+}, Cd^{2+} and Pb^{2+} for preconcentration in environmental samples prior to flame atomic absorption spectrometric determinations, J. Hazard. Mater. 159 (2008) 435–439.
[9] M. Ghaedi, Selective and sensitized spectrophotometric determination of trace amounts of Ni(II) ion using α-benzyl dioxime in surfactant media, Spectrochim. Acta, Part A 66 (2007) 295–301.
[10] M.C. Basso, E.G. Cerrella, A.L. Cukierman, Activated carbons developed from a rapidly renewable biosource for removal of cadmium(II) and nickel(II) Ions from dilute aqueous solutions, Ind. Eng. Chem. Res. 41 (2002) 180–189.
[11] C. Huang, Y.-C. Chung, M.-R. Liou, Adsorption of Cu(II) and Ni(II) by pelletized biopolymer, J. Hazard. Mater. 45 (1996) 265–277.
[12] W. Kaminski, E. Tomczak, K. Jaros, Interactions of metal ions sorbed on chitosan beads, Desalination 218 (2008) 281–286.
[13] M. Amini, H. Younesi, N. Bahramifar, Biosorption of nickel(II) from aqueous solution by *Aspergillus niger*: response surface methodology and isotherm study, Chemosphere 75 (2009) 1483–1491.
[14] S.R. Popuri, Y. Vijaya, V.M. Boddu, K. Abburi, Adsorptive removal of copper and nickel ions from water using chitosan coated PVC beads, Bioresour. Technol. 100 (2009) 194–199.
[15] B. Krajewska, Membrane-based processes performed with use of chitin/chitosan materials, Sep. Purif. Technol. 41 (2005) 305–312.
[16] L. Zhou, Y. Wang, Z. Liu, Q. Huang, Characteristics of equilibrium, kinetics studies for adsorption of Hg(II), Cu(II), and Ni(II) ions by thiourea-modified magnetic chitosan microspheres, J. Hazard. Mater. 161 (2009) 995–1002.
[17] C. Jeon, W.H. Höll, Chemical modification of chitosan and equilibrium study for mercury ion removal, Water Res. 37 (2003) 4770–4780.
[18] M.N.V. Ravi Kumar, A review of chitin and chitosan applications, React. Funct. Polym. 46 (2000) 1–27.
[19] D. Chauhan, N. Sankararamakrishnan, Highly enhanced adsorption for decontamination of lead ions from battery wastewaters using chitosan functionalized with xanthate, Bioresour. Technol. 99 (2008) 9021–9024.
[20] A.-H. Chen, S.-C. Liu, C.-Y. Chen, C.-Y. Chen, Comparative adsorption of Cu(II), Zn(II), and Pb(II) ions in aqueous solution on the crosslinked chitosan with epichlorohydrin, J. Hazard. Mater. 154 (2008) 184–191.
[21] J.R. Rangel-Mendez, R. Monroy-Zepeda, E. Leyva-Ramos, P.E. Diaz-Flores, K. Shirai, Chitosan selectivity for removing cadmium(II), copper(II), and lead(II) from aqueous phase: pH and organic matter effect, J. Hazard. Mater. 162 (2009) 503–511.
[22] N. Sankararamakrishnan, A.K. Sharma, R. Sanghi, Novel chitosan derivative for the removal of cadmium in the presence of cyanide from electroplating wastewater, J. Hazard. Mater. 148 (2007) 353–359.
[23] L. Qi, Z. Xu, Lead sorption from aqueous solutions on chitosan nanoparticles, Colloids Surf., A 251 (2004) 183–190.
[24] S. Haider, S.-Y. Park, Preparation of the electrospun chitosan nanofibers and their applications to the adsorption of Cu(II) and Pb(II) ions from an aqueous solution, J. Membr. Sci 328 (2009) 90–96.
[25] M.R. de Moura, F.A. Aouada, L.H.C. Mattoso, Preparation of chitosan nanoparticles using methacrylic acid, J. Colloid Interface Sci. 321 (2008) 477–483.
[26] R. Kumar, N.R. Bishnoi, K. Garima, Bishnoi, Biosorption of chromium(VI) from aqueous solution and electroplating wastewater using fungal biomass, Chem. Eng. J. 135 (2008) 202–208.
[27] J.C.P. Vaghetti, E.C. Lima, B. Royer, B.M. da Cunha, N.F. Cardoso, J.L. Brasil, S.L.P. Dias, Pecan nutshell as biosorbent to remove Cu(II), Mn(II) and Pb(II) from aqueous solutions, J. Hazard. Mater. 162 (2009) 270–280.
[28] O. Redlich, D.L. Peterson, A useful adsorption isotherm, J. Phys. Chem. 63 (1959), 1024-1024.
[29] K.S. Low, C.K. Lee, S.C. Liew, Sorption of cadmium and lead from aqueous solutions by spent grain, Process Biochem. 36 (2000) 59–64.
[30] Y.S. Ho, G. McKay, Pseudo-second order model for sorption processes, Process Biochem. 34 (1999) 451–465.
[31] C.-G. Liu, K.G.H. Desai, X.-G. Chen, H.-J. Park, Preparation and characterization of nanoparticles containing trypsin based on hydrophobically modified chitosan, J. Agric. Food. Chem. 53 (2005) 1728–1733.
[32] A.T. Paulino, J.I. Simionato, J.C. Garcia, J. Nozaki, Characterization of chitosan and chitin produced from silkworm crysalides, Carbohydr. Polym. 64 (2006) 98–103.
[33] G.S. Azhgozhinova, O. Güven, N. Pekel, A.V. Dubolazov, G.A. Mun, Z.S. Nurkeeva, Complex formation of linear poly(methacrylic acid) with uranyl ions in aqueous solutions, J. Colloid Interface Sci. 278 (2004) 155–159.
[34] Y.-H. Lin, C.-K. Chung, C.-T. Chen, H.-F. Liang, S.-C. Chen, H.-W. Sung, Preparation of nanoparticles composed of chitosan/poly-γ-glutamic and evaluation of their permeability through Caco-2 cells, Biomacromolecules 6 (2005) 1104–1112.
[35] J.-W. Wang, C.-Y. Chen, Y.-M. Kuo, Chitosan-poly(acrylic acid) nanofiber networks prepared by the doping induction of succinic acid and its ammonia-response studies, Polym. Adv. Technol. 19 (2008) 1343–1352.
[36] A.A. De Angelis, D. Capitani, V. Crescenzi, Synthesis and ^{13}C CP-MAS NMR characterization of a new chitosan-based polymeric network, Macromolecules 31 (1998) 1595–1601.
[37] Z. Huipeng, W. Lin, G. Yang, Q. Chen, Molecular weight effect on the complexation of poly(methacrylic acid) and poly(ethylene oxide) as studied by high-resolution solid-state ^{13}C NMR spectroscopy, Eur. Polym. J. 41 (2005) 2354–2359.
[38] H. Liu, F. Yang, Y. Zheng, J. Kang, J. Qu, J.P. Chen, Improvement of metal adsorption onto chitosan/*Sargassum* sp. composite sorbent by an innovative ion-imprint technology, Water Res. 45 (2011) 145–154.
[39] H. Zhu, J. Ji, R. Lin, C. Gao, L. Feng, J. Shen, Surface engineering of poly(D,L-lactic acid) by entrapment of chitosan-based derivatives for the promotion of chondrogenesis, J. Biomed. Mater. Res. 62 (2002) 532–539.
[40] J.P. Chen, L. Yang, Study of a heavy metal biosorption onto raw and chemically modified *Sargassum* sp. via spectroscopic and modeling analysis, Langmuir 22 (2006) 8906–8914.
[41] S. Hasan, T.K. Ghosh, D.S. Viswanath, V.M. Boddu, Dispersion of chitosan on perlite for enhancement of copper(II) adsorption capacity, J. Hazard. Mater. 152 (2008) 826–837.
[42] R.Y. Stefanova, Sorption of metal ions from aqueous solutions by thermally activated electroplating sludge, J. Environ. Sci. Health. Part A Toxic/Hazard. Subst. Environ. Eng. 35 (2000) 593–607.
[43] M.S. Dzul Erosa, T.I. Saucedo Medina, R. Navarro Mendoza, M. Avila Rodriguez, E. Guibal, Cadmium sorption on chitosan sorbents: kinetic and equilibrium studies, Hydrometallurgy 61 (2001) 157–167.
[44] E.P. Kuncoro, J. Roussy, E. Guibal, Mercury recovery by polymer-enhanced ultrafiltration: comparison of chitosan and poly(ethylenimine) used as macroligand, Sep. Sci. Technol. 40 (2005) 659–684.
[45] P. Chassary, T. Vincent, E. Guibal, Metal anion sorption on chitosan and derivative materials: a strategy for polymer modification and optimum use, React. Funct. Polym. 60 (2004) 137–149.
[46] A.T. Paulino, M.R. Guilherme, A.V. Reis, E.B. Tambourgi, J. Nozaki, E.C. Muniz, Capacity of adsorption of Pb^{2+} and Ni^{2+} from aqueous solutions by chitosan produced from silkworm chrysalides in different degrees of deacetylation, J. Hazard. Mater. 147 (2007) 139–147.
[47] S. Sen Gupta, K.G. Bhattacharyya, Immobilization of Pb(II), Cd(II) and Ni(II) ions on kaolinite and montmorillonite surfaces from aqueous medium, J. Environ. Manage. 87 (2008) 46–58.
[48] K.G. Sreejalekshmi, K.A. Krishnan, T.S. Anirudhan, Adsorption of Pb(II) and Pb(II)-citric acid on sawdust activated carbon: kinetic and equilibrium isotherm studies, J. Hazard. Mater. 161 (2009) 1506–1513.
[49] A. Sarl, M. Tuzen, Ö.D. Uluözlü, M. Soylak, Biosorption of Pb(II) and Ni(II) from aqueous solution by lichen (*Cladonia furcata*) biomass, Biochem. Eng. J. 37 (2007) 151–158.
[50] A.A. Atia, A.M. Donia, K.Z. Elwakeel, Adsorption behaviour of non-transition metal ions on a synthetic chelating resin bearing iminoacetate functions, Sep. Purif. Technol. 43 (2005) 43–48.
[51] K.H. Chu, Removal of copper from aqueous solution by chitosan in prawn shell: adsorption equilibrium and kinetics, J. Hazard. Mater. 90 (2002) 77–95.
[52] J. Chen, S. Yiacoumi, Biosorption of metal ions from aqueous solutions, Sep. Sci. Technol. 32 (1997) 51–69.

UNCORRECTED PROOF

[53] İ.A. Şengil, M. Özacar, Competitive biosorption of Pb^{2+}, Cu^{2+} and Zn^{2+} ions from aqueous solutions onto valonia tannin resin, J. Hazard. Mater. 166 (2009) 1488–1494.
[54] K.G. Bhattacharyya, A. Sharma, Adsorption of Pb(II) from aqueous solution by *Azadirachta indica* (Neem) leaf powder, J. Hazard. Mater. 113 (2004) 97–109.
[55] E. Guibal, M. Jansson-Charrier, I. Saucedo, P.L. Cloirec, Enhancement of metal ion sorption performances of chitosan: effect of the structure on the diffusion properties, Langmuir 11 (2002) 591–598.
[56] D. Nibou, H. Mekatel, S. Amokrane, M. Barkat, M. Trari, Adsorption of Zn^{2+} ions onto NaA and NaX zeolites: kinetic, equilibrium and thermodynamic studies, J. Hazard. Mater. 173 (2010) 637–646.
[57] B. Krajewska, Diffusion of metal ions through gel chitosan membranes, React. Funct. Polym. 47 (2001) 37–47.
[58] E. Guibal, Interactions of metal ions with chitosan-based sorbents: a review, Sep. Purif. Technol. 38 (2004) 43–74.
[59] G.M. Gadd, Biosorption: critical review of scientific rationale, environmental importance and significance for pollution treatment, J. Chem. Technol. Biotechnol. 84 (2009) 13–28.
[60] M. Özacar, I.A. Sengil, Adsorption of metal complex dyes from aqueous solutions by pine sawdust, Bioresour. Technol. 96 (2005) 791–795.
[61] Z. Rawajfih, N. Nsour, Thermodynamic analysis of sorption isotherms of chromium(VI) anionic species on reed biomass, J. Chem. Thermodyn. 40 (2008) 846–851.
[62] I. Langmuir, The constitution and fundamental properties of solids and liquids: Part I. Solids, J. Am. Chem. Soc. 38 (1916) 2221–2295.
[63] C.E. Zubieta, P.V. Messina, C. Luengo, M. Dennehy, O. Pieroni, P.C. Schulz, Reactive dyes remotion by porous TiO_2–chitosan materials, J. Hazard. Mater. 152 (2008) 765–777.
[64] M. Ozmen, K. Can, I. Akin, G. Arslan, A. Tor, Y. Cengeloglu, M. Ersoz, Surface modification of glass beads with glutaraldehyde: characterization and their adsorption property for metal ions, J. Hazard. Mater. 171 (2009) 594–600.
[65] J.C.Y. Ng, W.H. Cheung, G. McKay, Equilibrium studies for the sorption of lead from effluents using chitosan, Chemosphere 52 (2003) 1021–1030.
[66] S. Pradhan, S.S. Shukla, K.L. Dorris, Removal of nickel from aqueous solutions using crab shells, J. Hazard. Mater. 125 (2005) 201–204.
[67] A. Tor, Removal of fluoride from an aqueous solution by using montmorillonite, Desalination 201 (2006) 267–276.
[68] M.-W. Wan, I.G. Petrisor, H.-T. Lai, D. Kim, T.F. Yen, Copper adsorption through chitosan immobilized on sand to demonstrate the feasibility for in situ soil decontamination, Carbohydr. Polym. 55 (2004) 249–254.
[69] F.-C. Wu, R.-L. Tseng, R.-S. Juang, Kinetic modeling of liquid-phase adsorption of reactive dyes and metal ions on chitosan, Water Res. 35 (2001) 613–618.
[70] Ö. Gerçel, H.F. Gerçel, Adsorption of lead(II) ions from aqueous solutions by activated carbon prepared from biomass plant material of *Euphorbia rigida*, Chem. Eng. J. 132 (2007) 289–297.
[71] S.J. Allen, Q. Gan, R. Matthews, P.A. Johnson, Kinetic modeling of the adsorption of basic dyes by kudzu, J. Colloid Interface Sci. 286 (2005) 101–109.
[72] G.J. Cuello, G. Román-Ross, A. Fernández-Martínez, O. Sobolev, L. Charlet, N.T. Skipper, Pollutant speciation in water and related environmental treatment issues, neutron applications in Earth, Energy Environ. Sci. (2009) 491–520.
[73] A. Sarl, M. Tuzen, Biosorption of total chromium from aqueous solution by red algae (*Ceramium virgatum*): equilibrium, kinetic and thermodynamic studies, J. Hazard. Mater. 160 (2008) 349–355.
[74] F. Ghorbani, H. Younesi, S.M. Ghasempouri, A.A. Zinatizadeh, M. Amini, A. Daneshi, Application of response surface methodology for optimization of cadmium biosorption in an aqueous solution by *Saccharomyces cerevisiae*, Chem. Eng. J. 145 (2008) 267–275.
[75] M. Amini, H. Younesi, N. Bahramifar, A.A.Z. Lorestani, F. Ghorbani, A. Daneshi, M. Sharifzadeh, Application of response surface methodology for optimization of lead biosorption in an aqueous solution by *Aspergillus niger*, J. Hazard. Mater. 154 (2008) 694–702.
[76] M. Amini, H. Younesi, N. Bahramifar, Statistical modeling and optimization of the cadmium biosorption process in an aqueous solution using *Aspergillus niger*, Colloids Surf., A 337 (2009) 67–73.
[77] EPA, Effluent limitations guidelines, pretreatment standards, and new source performance standards: metal products and machinery; proposed rule, CFR Parts 433, 438, and 464, 1995, pp. 40.
[78] P. Baroni, R.S. Vieira, E. Meneghetti, M.G.C. da Silva, M.M. Beppu, Evaluation of batch adsorption of chromium ions on natural and crosslinked chitosan membranes, J. Hazard. Mater. 152 (2008) 1155–1163.
[79] S. Haider, S.-Y. Park, Preparation of the electrospun chitosan nanofibers and their applications to the adsorption of Cu(II) and Pb(II) ions from an aqueous solution, J. Membr. Sci. 328 (2009) 90–96.
[80] J.R. Evans, W.G. Davids, J.D. MacRae, A. Amirbahman, Kinetics of cadmium uptake by chitosan-based crab shells, Water Res. 36 (2002) 3219–3226.

UNCORRECTED PROOF